

**Supporting Information for**  
**Revealing the different effects of VIB transition metal X (X = Cr, Mo,**  
**W) on the electrochemical performance of Li-rich cathode  $\text{Li}_2\text{MnO}_3$**   
**by first-principles calculations**

Shiwei Zhang<sup>a</sup>, Jianchuan Wang<sup>a,\*</sup>, Huan Liu<sup>b</sup>, Weibin Zhang<sup>b</sup>, Lixian Sun<sup>c</sup>, Yong Du<sup>a</sup>, Hans J Seifert<sup>d</sup>, Ting Lei<sup>a</sup>

<sup>a</sup> State Key Laboratory of Powder Metallurgy, Central South University, 410083, Changsha

<sup>b</sup> Key Laboratory for Liquid-Solid Structural Evolution and Processing of Materials (Ministry of Education), Shandong University, 250061, Jinan, China

<sup>c</sup> Guangxi Key Laboratory of Information Materials, Guilin University of Electronic Technology, 541004, Guilin, China

<sup>d</sup> Institute for Applied Materials, Karlsruhe Institute of Technology, Germany

Corresponding author: \* jcw728@126.com

**Table S1.** The energies of  $\text{Li}_2\text{MnO}_3$  with different magnetic configurations.

Magnetic configuration	Energy (eV/f.u.)
ferromagnetic	-37.1728
antiferromagnetic	-37.1642

**Table S2.** Lattice parameters and volumes of  $\text{Li}_2\text{MnO}_3$  and  $\text{Li}_2\text{MnO}_3$  with Cr, Mo and W dilute doping.

System	Lattice parameter ( $\text{\AA}$ )			Volume ( $\text{\AA}^3$ )
	a	b	c	
$\text{Li}_2\text{MnO}_3$	5.010	8.660	5.091	208.223
Cr- $\text{Li}_2\text{MnO}_3$	5.015	8.659	5.094	208.441
Mo- $\text{Li}_2\text{MnO}_3$	5.040	8.690	5.107	210.642
W- $\text{Li}_2\text{MnO}_3$	5.036	8.729	5.104	211.633

**Table S3.** The average Bader charges of doped TM, Mn and O near the TM in TM- $\text{Li}_x\text{MnO}_3$  (TM = Cr, Mo, W) systems.

System	$x$	Average Bader charge (e)		
		Mn	O	TM (Cr, Mo, W)
$\text{Li}_x\text{MnO}_3$	2	+1.897	-1.226	+1.897
	1.75	+1.903	-1.066	+1.899
	1.5	+1.928	-0.975	+1.928
	1.25	+1.940	-0.991	+1.938
	1	+1.960	-0.954	+1.960
Cr- $\text{Li}_x\text{MnO}_3$	2	+1.897	-1.234	+1.982
	1.75	+1.912	-1.034	+2.131
	1.5	+1.933	-0.984	+2.115
	1.25	+1.928	-0.993	+2.145
	1	+1.958	-0.933	+2.117
Mo- $\text{Li}_x\text{MnO}_3$	2	+1.867	-1.294	+2.544
	1.75	+1.889	-1.132	+2.726
	1.5	+1.917	-1.087	+2.732
	1.25	+1.918	-1.104	+2.725
	1	+1.973	-1.066	+2.747
W- $\text{Li}_x\text{MnO}_3$	2	+1.779	-1.264	+2.962
	1.75	+1.889	-1.177	+2.999
	1.5	+1.914	-1.136	+3.003
	1.25	+1.918	-1.149	+2.985
	1	+1.952	-1.112	+3.001

**Table S4.** The average formation enthalpies of different Li vacancies in fully lithiated

Li<sub>2</sub>MnO<sub>3</sub> and TM-Li<sub>2</sub>MnO<sub>3</sub>(TM=Cr, Mo, W)

System	Site	Formation enthalpy (eV)
Li <sub>2</sub> MnO <sub>3</sub>	2 <i>b</i>	4.78
	2 <i>c</i>	4.67
	4 <i>h</i>	4.62
Cr-Li <sub>2</sub> MnO <sub>3</sub>	2 <i>b</i>	4.30
	2 <i>c</i>	4.21
	4 <i>h</i>	4.18
Mo-Li <sub>2</sub> MnO <sub>3</sub>	2 <i>b</i>	2.89
	2 <i>c</i>	2.79
	4 <i>h</i>	2.75
W-Li <sub>2</sub> MnO <sub>3</sub>	2 <i>b</i>	2.55
	2 <i>c</i>	2.43
	4 <i>h</i>	2.43

**Table S5.** The average formation enthalpies of O vacancies around TM at different delithiation stages in TM-Li<sub>2</sub>MnO<sub>3</sub>(TM=Cr, Mo, W)

System	$x$	Average formation enthalpy (eV)
$\text{Li}_x\text{MnO}_3$	2	2.59
	1.75	0.45
	1.5	0.10
	1.25	-0.07
	1	-0.63
$\text{Cr-Li}_x\text{MnO}_3$	2	2.46
	1.75	-0.18
	1.5	-0.28
	1.25	-0.53
	1	-1.20
$\text{Mo-Li}_x\text{MnO}_3$	2	3.40
	1.75	1.26
	1.5	0.29
	1.25	0.04
	1	-0.74
$\text{W-Li}_x\text{MnO}_3$	2	3.71
	1.75	1.68
	1.5	0.68
	1.25	0.44
	1	-0.56

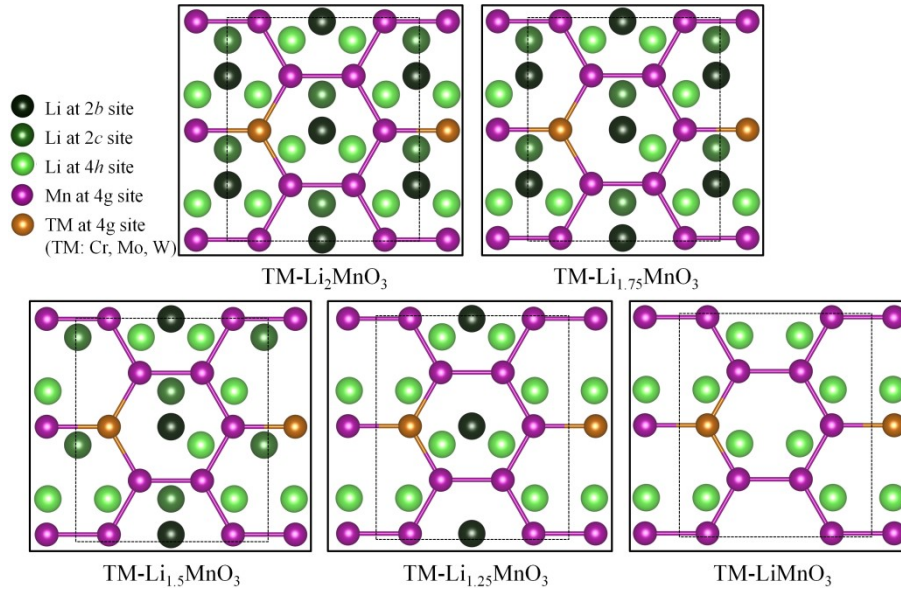


**Figure S1.** Illustrations of the partially delithiated structures of TM-Li<sub>*x*</sub>MnO<sub>3</sub> (*x* = 2, 1.75, 1.5, 1.25, 1). The black dashed box represents a structural period. The delithiation sequence is described as follows: (1) some Li ions at the 4*h* sites are extracted ( $1.75 \leq x < 2$ ), (2) some Li ions at the 2*b* sites are extracted ( $1.5 \leq x < 1.75$ ), (3) half of the Li ions at the 2*c* sites are extracted and the other half of Li ions at the 2*c* sites migrate to the 4*h* sites ( $1.25 \leq x < 1.5$ ), (4) all Li ions at the 2*b* sites are extracted ( $1 \leq x < 1.25$ ).

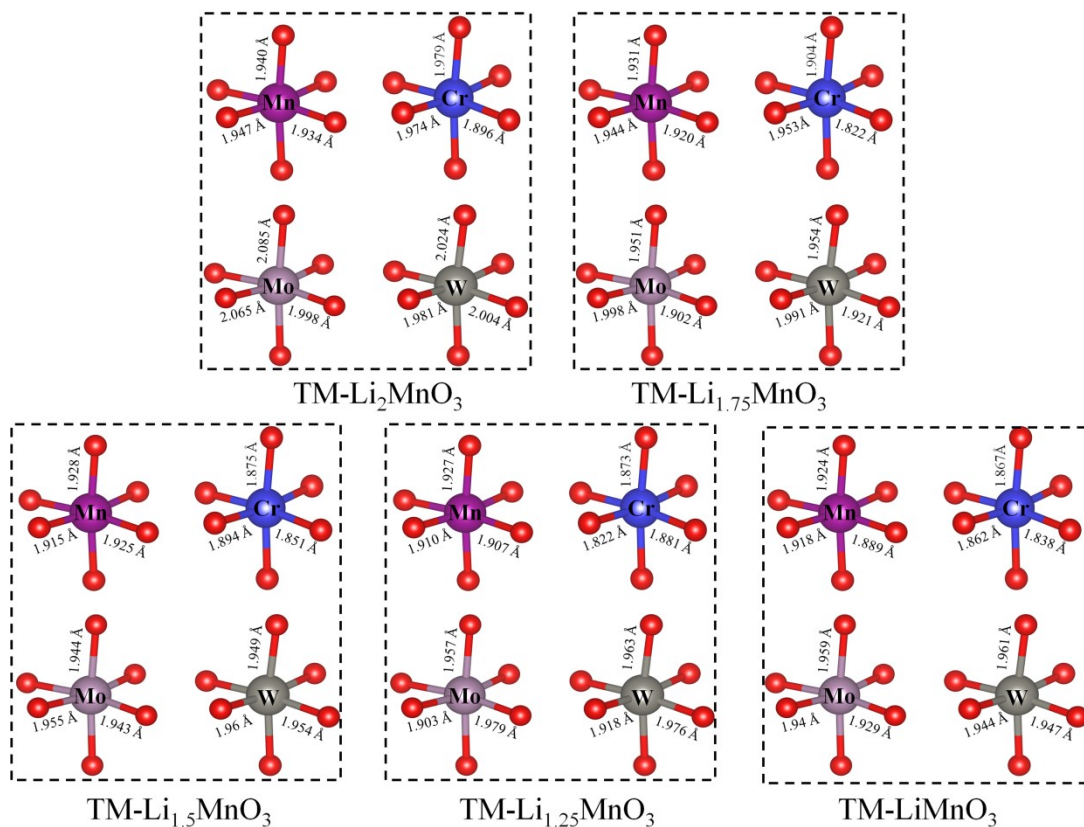


**Figure S2.** The Bond lengths of TM-O at different stages of delithiation of  $\text{TM-Li}_x\text{MnO}_3$  ( $x = 2, 1.75, 1.5, 1.25, 1$ ).



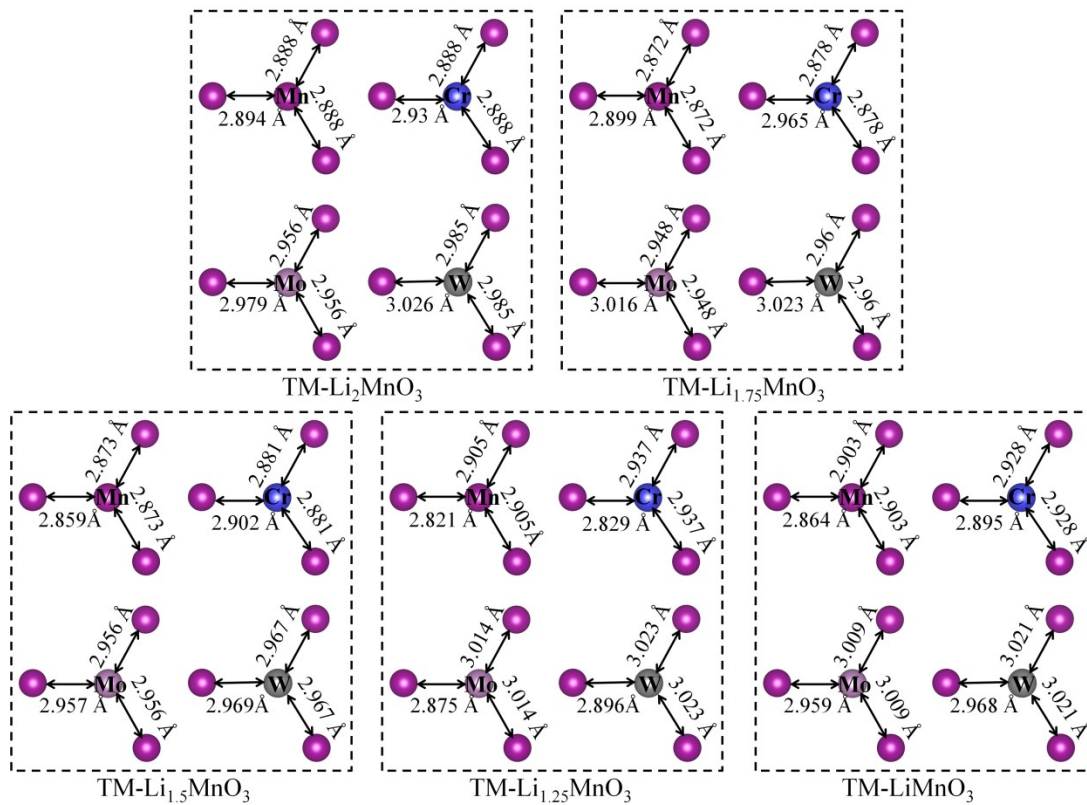


**Figure S3.** The distances between TM and its surrounding Mn at different stages of delithiation of  $\text{TM-Li}_x\text{MnO}_3$  ( $x = 2, 1.75, 1.5, 1.25, 1$ ).

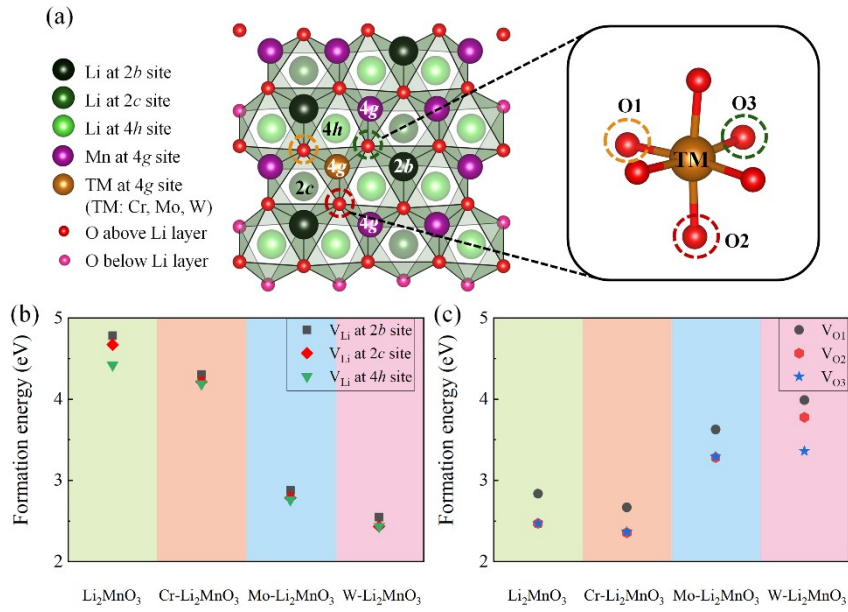


**Figure S4.** (a) Illustrations of the nearest Li and O sites near the TM doping site in TM-Li<sub>2</sub>MnO<sub>3</sub> (TM=Cr, Mo, W). (b) Formation enthalpies of different Li vacancies in TM-Li<sub>2</sub>MnO<sub>3</sub>. (c) Formation enthalpies of different O vacancies in TM-Li<sub>2</sub>MnO<sub>3</sub>.

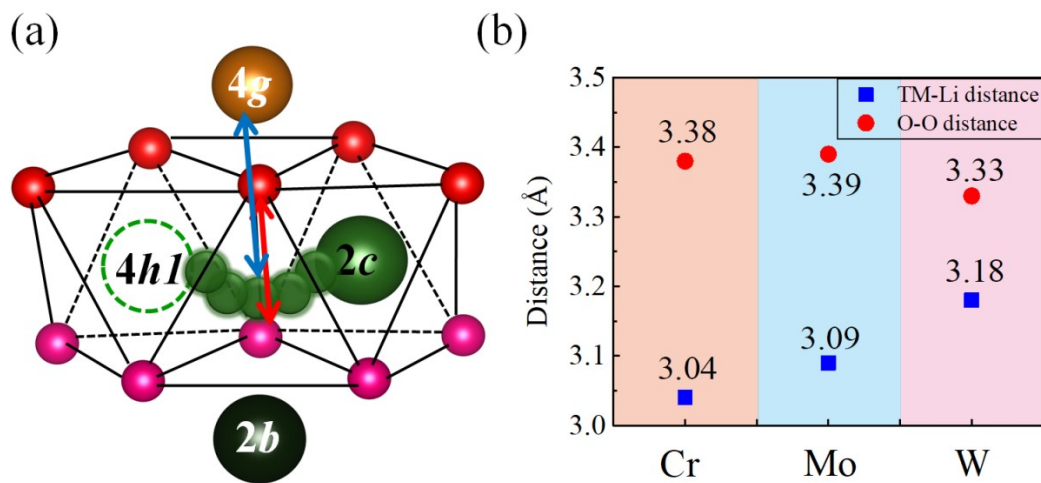


**Figure S5.** (a) Illustrations of the maximum distance between the mobile Li and TM in path 2c - 4h1 (shown by the blue arrow), and the maximum distance between O in O-O dumbbell structure (shown by the red arrow). (b) The values of the distances.